European Heart Journal (2006) **27**, 2833–2839
doi:10.1093/eurheartj/ehl358

Septal ablation in hypertrophic obstructive cardiomyopathy improves systolic myocardial function in the lateral (free) wall: a follow-up study using CMR tissue tagging and 3D strain analysis

Willem G. van Dockum[1]*, Joost P.A. Kuijer[2], Marco J.W. Götte[1], Folkert J. ten Cate[3], Jurrien M. ten Berg[4], Aernout M. Beek[1], Jos W.R. Twisk[5], Johannes Tim Marcus[2], Cees A. Visser[1], and Albert C. van Rossum[1]

[1] *Department of Cardiology, VU University Medical Center, De Boelelaan 1117, PO Box 7057, 1081 HV Amsterdam, The Netherlands;* [2] *Department of Physics and Medical Technology, VU University Medical Center, Amsterdam, The Netherlands;* [3] *Department of Cardiology, Thoraxcenter Erasmus Medical Center, Rotterdam, The Netherlands;* [4] *Department of Cardiology, St Antonius Hospital, Nieuwegein, The Netherlands; and* [5] *Department of Clinical Epidemiology and Biostatistics, VU University Medical Center, Amsterdam, The Netherlands*

Received 1 March 2006; revised 12 October 2006; accepted 19 October 2006; online publish-ahead-of-print 10 November 2006

See page 2746 for the editorial comment on this article (doi:10.1093/eurheartj/ehl324)

KEYWORDS
Hypertrophy;
Cardiomyopathy;
Myocardial ablation;
Tagging;
Magnetic resonance imaging

Aims Alcohol septal ablation (ASA) has been successful in the treatment of symptomatic hypertrophic obstructive cardiomyopathy (HOCM). The aim of this study is to evaluate the effects of ethanol-induced myocardial infarcts on regional myocardial function using cardiac magnetic resonance (CMR) tissue tagging and 3-dimensional (3D) strain analysis.
Methods and results In nine patients (age 52 ± 15 years) who underwent ASA, CMR was performed prior to and 6 months after the procedure. Regional myocardial mass was evaluated using cine imaging. Myocardial tagging was used to calculate systolic 3D myocardial strain values. These strain values were used to calculate the shortening index (SI), a robust parameter for myocardial contraction. Maximum end-systolic (ES) SI and systolic SI rate were quantified in three circumferential segments: septum, adjacent, and remote (lateral) myocardium. Compared with baseline, septal and non-septal mass decreased at follow-up (from 72 ± 27 to 59 ± 21 g; $P = 0.008$ and from 131 ± 34 to 109 ± 30 g; $P = 0.008$, respectively). In the septum, maximum ES SI and SI rate remained unchanged after ASA. In adjacent myocardium, ES SI remained unchanged, whereas SI rate improved (from −56.5 ± 21.1 to −70.0 ± 16.7%/s; $P = 0.02$). Both ES SI and SI rate improved significantly in remote myocardium (from −16.9 ± 2.8 to −18.8 ± 3.2%; $P = 0.02$ and from −70.3 ± 9.2 to −86.1 ± 15.0%/s; $P = 0.01$, respectively).
Conclusion Reduction of left ventricular (LV) outflow tract obstruction in symptomatic HOCM is associated with a significant reduction in myocardial mass and improvement of intramural systolic function in the lateral (remote) wall, indicating reversed LV remodelling.

Introduction

Recently, alcohol septal ablation (ASA) has been successfully introduced to treat symptomatic patients with hypertrophic obstructive cardiomyopathy (HOCM).[1–5] Ablation by ethanol infusion into septal branches of the left anterior descending coronary artery results in an artificially induced septal myocardial infarction with regional myocardial wall thinning, a decrease of the pressure gradient and left ventricular (LV) wall stress, and subsequently a relief of symptoms.[6–9]

Using cardiac magnetic resonance (CMR) imaging, we have demonstrated that both septal and non-septal (remote) myocardial mass reduction can be found as early as 1 month after ASA in patients with HOCM, and mass reduction continues afterwards.[10,11] The reduction in remote LV mass supports the theory that myocardial hypertrophy in HOCM is not exclusively caused by the genetic disorder, but is also afterload-dependent and reversible. Few studies report on the effects of afterload reduction on regional myocardial function in these patients. The reduction of the Tei index, an echocardiographic Doppler parameter reflecting both systolic and diastolic LV functions, was found, suggesting improved myocardial performance.[12] Echocardiographic strain rate imaging has shown reduced systolic function in

* Corresponding author. Tel: +31 20 4442244; fax: +31 20 4442446.
E-mail address: wg.vandockum@vumc.nl

the peri-infarct septal zone and preserved systolic function in the remote non-ischaemic septal zone directly after ASA.[13]

CMR tissue tagging with three-dimensional (3D)-strain analysis is an established method for quantification of regional myocardial function.[14–16] When the technique is used in patients with myocardial infarction because of coronary artery disease, differences in function between infarcted and non-infarcted (remote) regions can be detected accurately. These regional differences in function are thought to play a role in post-infarct remodelling.[17,18] However, it is unknown to what extent a therapeutic and artificially induced infarction affects regional function in patients with obstructive cardiomyopathy with an associated pre-existent abnormal structure of the myocardium. On the one hand, the ethanol-induced infarction may cause a further decline in regional myocardial function and trigger an adverse remodelling process. On the other hand, beneficial effects due to the reduction of the pressure gradient might counterbalance deleterious effects from ASA.

The purpose of this study is to determine the effect of ASA on regional myocardial function. Three-dimensional myocardial strain was quantified in nine patients with symptomatic HOCM before and 6 months after successful ASA.

Methods

Patients

The study protocol was approved by the Committee on Research Involving Human Subjects and by the Medical Ethics Committee of the VU University Medical Center, Amsterdam, The Netherlands. Consecutive patients with HOCM scheduled for ASA and eligible for CMR imaging were studied. Exclusion criteria were any absolute or relative contraindication to MR imaging (e.g. pacemaker and claustrophobia), atrial fibrillation (AF), or failure to give informed consent. The indication for ASA was based on a significant LV outflow tract (LVOT) pressure gradient as documented by echocardiography and symptoms [New York Heart Association (NYHA) functional classes II–IV], despite medical treatment. The septal ablation procedure has been described previously.[10]

One patient was excluded for enrolment because of AF. In total, 19 consecutive patients underwent 3D CMR myocardial tagging in addition to a standard CMR imaging protocol that included volume and mass measurements and delayed contrast-enhanced (DCE) imaging. Four patients were lost to 6 months follow-up: three required pacemaker implantation because of the development of complete atrioventricular block (in one patient, 3 months after the procedure) and one declined to return for the follow-up examination. Two patients with recurrent symptoms were excluded from the final analysis because no successful gradient reduction ($>$50%) was achieved after the septal ablation procedure. One of these patients underwent a redo procedure, and the other underwent a surgical myectomy in combination with mitral leaflet extension because the patient had an enlarged anterior mitral valve leaflet with residual systolic anterior motion and severe mitral regurgitation. In four patients, strain analysis was not possible because of poor image quality: in one patient, breath-holding was inadequate, one patient developed claustrophobia during the follow-up CMR, one patient had motion artefacts on FU CMR, and in one patient, tag lines faded very quickly. Results of the standard CMR protocol in a larger group (29 patients) have been published elsewhere.[11] This article reports the results of the subgroup that underwent CMR tagging.

Echocardiography

The LVOT pressure gradient was documented by Doppler echocardiography. In symptomatic patients, a pressure gradient of $\geq$50 mmHg at rest was considered to be significant. One patient with a resting gradient of $<$50 mmHg was symptomatic. In this patient, provocation was applied using the Valsalva manoeuvre, resulting in a pressure gradient of $\geq$50 mmHg.

CMR image acquisition

CMR was performed prior to and 6 months after ASA on a 1.5 T clinical scanner (Sonata, Siemens, Erlangen, Germany), using a four-element phased-array receiver coil. All images were acquired with ECG gating and during repeated single breath-holds of 10–15 s depending on heart rate.

Cine images were acquired using a segmented steady-state free precession gradient-echo sequence in three long-axis views (2-, 3-, and 4-chamber view) and in multiple short-axis views every 10 mm, covering the entire LV from base to apex.

DCE images were acquired 15–20 min after intravenous administration of 0.2 mmol/kg gadolinium-diethylene-triamine pentaacetic acid (DTPA) in the same views used in cine CMR, using a two-dimensional segmented inversion-recovery prepared gradient-echo sequence.[19] The DCE images were acquired in five patients at baseline and in all patients at follow-up CMR and were used to make sure that the ablation procedure was successful and that the infarct region was limited to the septum.[10]

CMR tissue tagging using spatial modulation of magnetization[15,16] was applied to create markers (tags) non-invasively within the myocardium for the calculation of myocardial strain. Five to six parallel LV short-axis- and three long-axis-tagged images were acquired by a spoiled gradient echo sequence. A temporal resolution of 30 ms was achieved by application of a view-sharing technique.

CMR image analysis

Analysis of cine images (global ventricular function)

Global LV function parameters, including end-diastolic volume (EDV), end-systolic volume (ESV), ejection fraction (EF), and total and septal myocardial mass, were quantified using the MASS software package (MEDIS, Leiden, The Netherlands). Endocardial and epicardial borders were traced manually in end-diastolic and ES frames of all short-axis slices. Papillary muscles were included in the assessment of LV mass. The septum was defined as the myocardium between the anterior and the posterior junctions of the right ventricle (RV) to the LV.

Analysis of tagged images (regional myocardial function)

The short-axis- and long-axis-tagged images were processed using a dedicated software package (SPAMMVU, University of Pennsylvania, PA, USA).[20] After combining the short-axis and long-axis myocardial motions, tetrahedrons (of myocardium) were created and the 3D strain values of these tetrahedrons were calculated.[21] The normal strains were expressed in a cardiac coordinate system defined by the radial, circumferential, and longitudinal directions. The strain components were computed with respect to these three directions.

The radial strain is defined as the relative change in the length of a radial line segment and expressed in per cent value. Positive radial strains represent the local contribution to wall thickening. Negative values for radial strain imply local wall thinning. Circumferential and longitudinal strains were defined similar to the radial strain, quantifying the change in length in the circumferential and longitudinal directions, respectively. Negative circumferential and longitudinal strains represent local shortening. From each strain parameter, peak values were determined and expressed as 'maximum systolic strain'.

Systolic strain rate was defined as the slope of the strain curve averaged from five time frames (from 90 to 210 ms after the QRS interval), reflecting myocardial deformation over time.

The circumferential–longitudinal shear strain gives the change in the angle between the circumferential and longitudinal line segments. This circumferential–longitudinal shear angle can be interpreted as the local contribution to global LV torsion.

The shortening index (SI) reflects the geometric mean of fractional one-dimensional shortening within the circumferential–longitudinal plane. The SI is negative for muscle shortening and directionally insensitive within the plane. SI turns out to be a robust parameter to quantify myocardial contraction.[22]

Strain values were averaged from base to apex, and strain parameters were calculated in six circumferential segments; anterior, antero-lateral, postero-lateral, inferior, infero-septal, and antero-septal. The infero- and antero-septal segments were considered to be target areas for the ethanol-induced myocardial infarction. The anterior and inferior segments were considered as 'adjacent' myocardium and the antero- and postero-lateral segments as 'remote' area.

Statistical analysis

Results are expressed as mean ± SD. Non-parametric testing (Wilcoxon signed rank test) was used to evaluate the changes in LV volumes, in global and regional myocardial mass, and in segmental strain values before and 6 months after ASA. All tests were two-sided and the data were aggregated on the patient level. Linear regression analysis was used to analyse the relationship between percentage of remote mass reduction and improvement of the SI.

All statistical analyses were performed with SPSS version 11.0, and significance was set at a value of $P \leq 0.05$.

Results

Mean age was 49 ± 19 years (range 18–71, five males). Nine patients received one or more drugs [beta-blocker ($n = 4$), calcium-channel blockers ($n = 7$), or anti-arrhythmic drugs ($n = 2$)]. After ASA, the dose-regimen in patients using a beta-blocker was continued; in two of the four patients receiving both calcium-channel blockers and beta-blockers pre-ablation, the calcium-channel blockers were discontinued at follow-up. During the ablation procedure, ethanol was injected in one septal artery in all patients. The mean volume of ethanol injected during the ASA procedure was 4.1 ± 1.4 mL (range 2.0–5.0 mL). The mean peak CK and CK-MB release were 1881 ± 831 U (range 991–3366) and 249 ± 103 U (range 100–376), respectively. In five patients, contrast-enhanced imaging was performed at baseline. In four patients, small patchy areas of hyperenhanced myocardium were observed in the ventricular wall and predominantly at the junctions of the RV and LV free walls. None of the patchy areas were transmural, and no hyperenhancement was observed in the antero- and postero-lateral segments (remote area). The number of focal areas of hyperenhancement per patient was 4.7 ± 1.0, representing an average mass of 0.5 ± 0.5 g per area. Using DCE imaging after the procedure, none of the patients had evidence of infarct-related hyperenhancement outside the interventricular septum. An example of the infarcted area as imaged by DCE is shown in *Figure 1*.

The dynamic pressure gradient decreased from 91 ± 15 to 11 ± 15 mmHg at 6 months after the procedure ($P < 0.001$). All patients reported subjective improvement of exercise tolerance. The mean NYHA functional class improved significantly from 2.8 ± 0.4 to 1.3 ± 0.5 ($P < 0.001$) at 6 months of follow-up.

Global ventricular function

Regional wall thickness, LV volumes, EF, and mass are summarized in *Table 1*. The decrease in regional wall thickness in the infarcted, adjacent, and remote myocardium was significant in all three regions. A significant mass reduction was observed both in the target septal myocardium and in the non-septal myocardium (both $P = 0.008$).

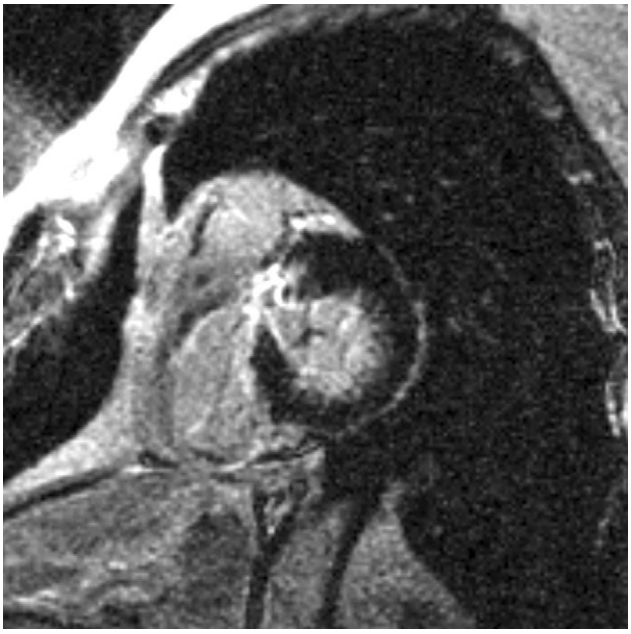

Figure 1 DCE image in a short-axis view. Hyperenhancement in the interventricular septum indicates the procedure-related infarct.

Regional myocardial function

Systolic strain

Figure 2 shows an example of ES short-axis-tagged images at baseline and 6 months after the septal ablation procedure. *Figure 3* represents a 3D functional display of circumferential shortening (E_{cc}), computed from five short-axis- and three long-axis-tagged views at baseline and at 6 months of follow-up. Three-dimensional strain parameters are listed in *Table 2*. Before ASA, myocardial function in the target septal area was significantly reduced when compared with the remote myocardium (for SI, −9.7 ± 4.2 vs. −16.9 ± 2.8; $P = 0.008$). After the artificially induced septal infarction, no significant changes of maximum systolic strain were observed in the septum.

In the adjacent myocardium, radial stretch and longitudinal shortening improved significantly ($P = 0.02$ and 0.01, respectively), whereas circumferential shortening remained unchanged. There was a trend in the improvement of the SI, although it did not reach statistical significance.

In the remote area, significant improvement in myocardial shortening was observed, reflected by the improved SI (from −16.9 ± 2.8 to −18.8 ± 3.2; $P = 0.017$). Both circumferential shortening and longitudinal shortening improved significantly ($P = 0.049$ and 0.041, respectively), whereas radial stretch remained unchanged.

Systolic strain rates at baseline vs. follow-up

Before ASA, systolic strain rate in the septal target area was significantly lower when compared with that in the adjacent and remote areas (both $P = 0.011$) *Figure 4*. Six months after the ablation procedure, systolic strain rates in the infarct area did not change compared with baseline

Table 1 Cardiac dimensions and mass at baseline and after ASA

	Baseline	6 months follow-up	Δ-value	*P*-value
IVS thickness at infarct site (mm)	19.9 ± 2.6	9.8 ± 2.6	10.1 ± 5.3	0.008
Wall thickness at mid LV level (mm)				
Septal wall	17.3 ± 5.5	15.3 ± 5.8	2.0 ± 1.8	0.02
Anterior wall	9.8 ± 3.8	8.8 ± 3.8	1.0 ± 0.9	0.011
Lateral wall	7.3 ± 1.1	6.3 ± 1.0	1.0 ± 0.9	0.011
Inferior wall	9.9 ± 4.0	9.1 ± 3.9	0.8 ± 0.7	0.02
LV EDV (mL)	160 ± 42	160 ± 36	0.4 ± 16	0.86
LV ESV (mL)	51 ± 16	55 ± 18	−3.7 ± 9	0.17
Stroke volume (mL)	109 ± 26	104 ± 21	4.8 ± 14	0.34
LVEF (%)	68 ± 3	66 ± 5	2.2 ± 5	0.33
Total LV mass (g)	203 ± 59	168 ± 50	34.9 ± 16	0.008
Septal mass (g)	72 ± 27	59 ± 21	13.1 ± 7	0.008
Non-septal mass (g)	131 ± 34	109 ± 30	21.8 ± 11	0.008

Values expressed as mean ± SD. Δ, actual changes from baseline at 6-month follow-up.

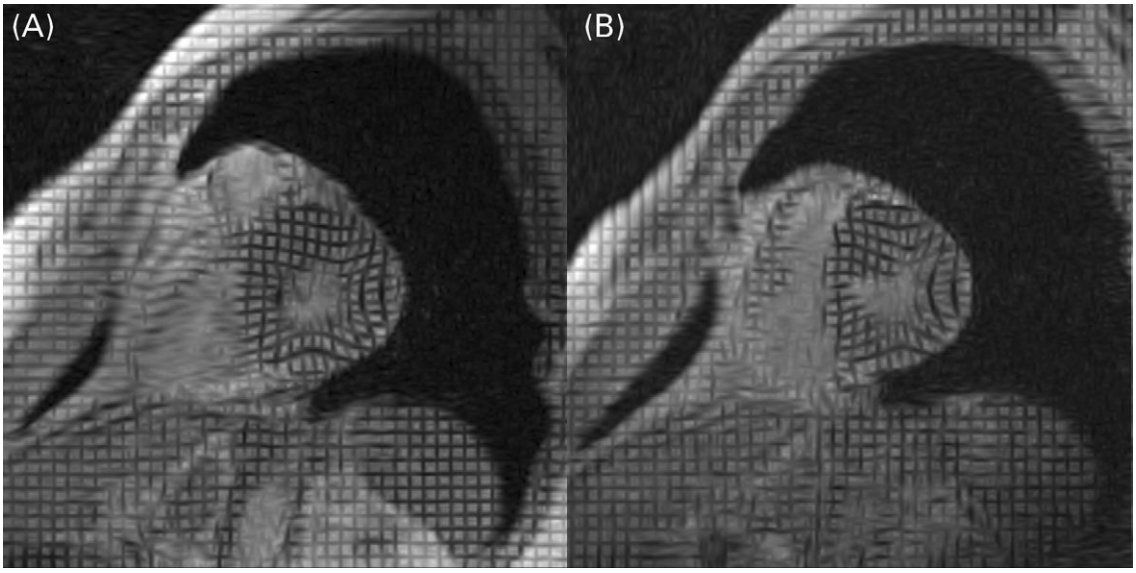

Figure 2 ES short-axis-tagged CMR images in an HOCM patient at baseline (*A*) and at 6 months after ASA (*B*).

(*Table 3*). However, in adjacent myocardium, all strain rates except the circumferential shortening strain rate increased. In remote myocardium, strain rates for all strain parameters except for the circumferential–longitudinal shear strain increased at follow-up (*Table 3*).

Correlation between remote mass reduction and SI

Linear regression analysis showed a strong positive correlation (not statistically significant) between per cent reduction of non-septal mass and per cent improvement in SI in remote myocardium at 6 months of follow-up ($r = 0.61$, $P = 0.08$).

Discussion

This is the first study that used CMR tissue tagging and 3D-strain analysis to evaluate the effects on regional myocardial function in symptomatic patients with HOCM after ASA. As reported previously, both septal and non-septal myocardial mass significantly decreased as early as 1 month after septal ablation and progressed on mid-term follow-up.[10,11] This reduction in non-septal LV mass supports the concept that myocardial hypertrophy in HOCM is partly afterload-dependent and reversible. Using CMR tissue tagging, we have now demonstrated that ASA improves regional intramural myocardial systolic function in the adjacent and remote myocardium. Both observations support the concept that a reduction of LVOT obstruction in symptomatic HOCM leads to reversed LV remodelling after ASA. The observed positive correlation between the percentage remote mass reduction and the improvement of remote myocardial contraction supports the hypothesis of a reversed remodelling process, although statistical significance could not be reached, which may be related to the relatively small sample size of the study population.

Effect of ASA on myocardial mass

Although HCM is a genetic disorder leading to a primary molecular abnormality resulting in an increase of wall thickness, elimination of the LVOT obstruction will result in a decrease of LV pressure and wall stress and subsequently

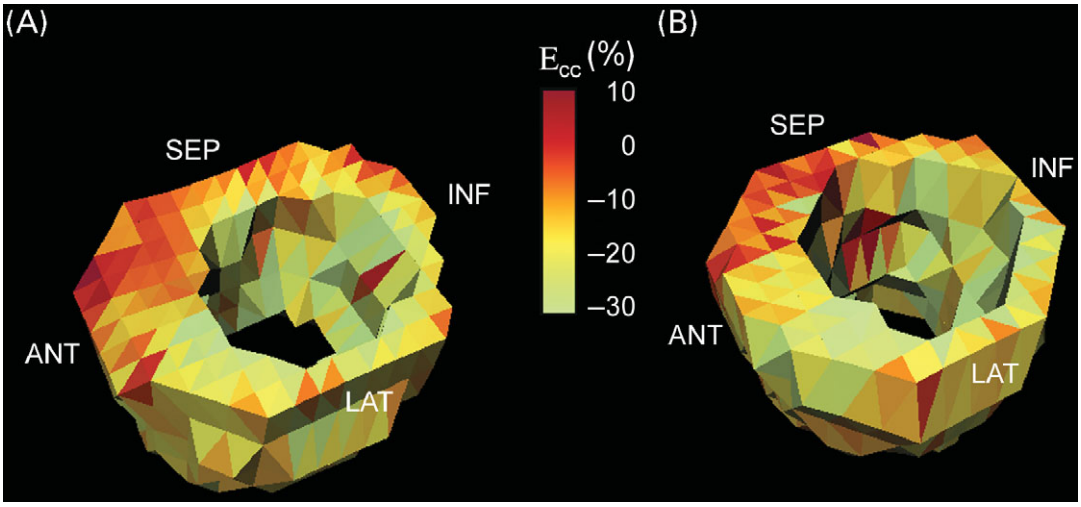

Figure 3 3D functional display of circumferential shortening (E_{cc}), calculated from five short-axis and three long-axis views at baseline (*A*) and at 6 months after ASA (*B*).

Table 2 Maximum systolic strains in septal, adjacent, and remote myocardium before and 6 months after ASA in HOCM

Maximum systolic strains	Baseline	Follow-up	Δ-value	*P*-value
Septum (antero- and inferoseptal wall)				
Radial stretch (Err)	10.3 ± 5.9	9.9 ± 5.0	0.4 ± 5.9	0.722
Circumferential shortening (Ecc)	−10.8 ± 3.6	−11.0 ± 3.0	0.2 ± 1.3	0.672
Longitudinal shortening (Ell)	−7.6 ± 4.4	−8.7 ± 3.8	1.1 ± 2.5	0.172
Torsion (Acl) (degrees)	7.4 ± 3.1	7.0 ± 3.4	0.4 ± 1.6	0.594
SI	−9.7 ± 4.2	−10.2 ± 3.5	0.5 ± 1.8	0.587
Adjacent (anterior and inferior wall)				
Radial stretch (Err)	15.0 ± 5.4	18.0 ± 4.2	3.0 ± 2.8	0.021
Circumferential shortening (Ecc)	−15.6 ± 5.5	−16.4 ± 4.1	0.8 ± 2.9	0.528
Longitudinal shortening (Ell)	−8.0 ± 4.0	−10.6 ± 3.9	2.6 ± 1.8	0.011
Torsion (Acl) (degrees)	8.2 ± 2.8	8.4 ± 2.1	0.2 ± 1.9	0.767
SI	−12.1 ± 4.8	−13.6 ± 3.7	1.4 ± 2.3	0.075
Remote (antero- and inferolateral wall)				
Radial stretch (Err)	25.5 ± 4.6	27.9 ± 5.6	2.4 ± 4.4	0.137
Circumferential shortening (Ecc)	−22.1 ± 3.6	−23.5 ± 3.3	1.5 ± 2.0	0.050
Longitudinal shortening (Ell)	−11.2 ± 3.3	−13.5 ± 4.5	2.3 ± 3.0	0.041
Torsion (Acl) (degrees)	8.3 ± 2.1	8.8 ± 1.3	0.5 ± 2.5	0.859
SI	−16.9 ± 2.8	−18.8 ± 3.2	1.8 ± 1.8	0.017

Values expressed as mean ± SD. Δ, actual changes from baseline at 6-month follow-up.

in a regression of LV hypertrophy. Accordingly, previous echocardiographic studies have demonstrated a significant reduction in LV mass at 1 year after septal ablation. This was not only due to thinning of the septal myocardium, but also due to a decrease in wall thickness throughout the LV circumference.[23] Using CMR, we demonstrated that reversed LV remodelling after ASA was associated with septal infarct location and correlated with reduction of the LVOT pressure gradient.[11] On the basis of these findings, it was concluded that myocardial hypertrophy in HOCM is at least in part afterload-dependent and reversible and not exclusively caused by the genetic disorder.

Effect of ASA on regional myocardial function

In patients with hypertrophic cardiomyopathy, it has been previously demonstrated that circumferential and longitudinal shortening is decreased in the septal, anterior, and inferior (hypertrophied) myocardial segments, compared with normal subjects.[24–26] Our 3D-strain data acquired prior to the ablation procedure are in line with these observations.

Compared with baseline, systolic myocardial strains and systolic strain rates in the target septal myocardium did not change after ASA. Prior to intervention, septal systolic deformation was already markedly reduced, and the formation of scar tissue as a result of the ethanol-ablation procedure did not lead to further impairment of the regional septal function. In contrast, Abraham *et al*.[13] found reduced systolic function in the peri-infarct septal zone and preserved systolic function in the non-ischaemic septal zone after septal ablation, using strain rate imaging with echocardiography. These findings are not contradictory to the present results because, first, in our study, the strain analysis was calculated for the whole septum without

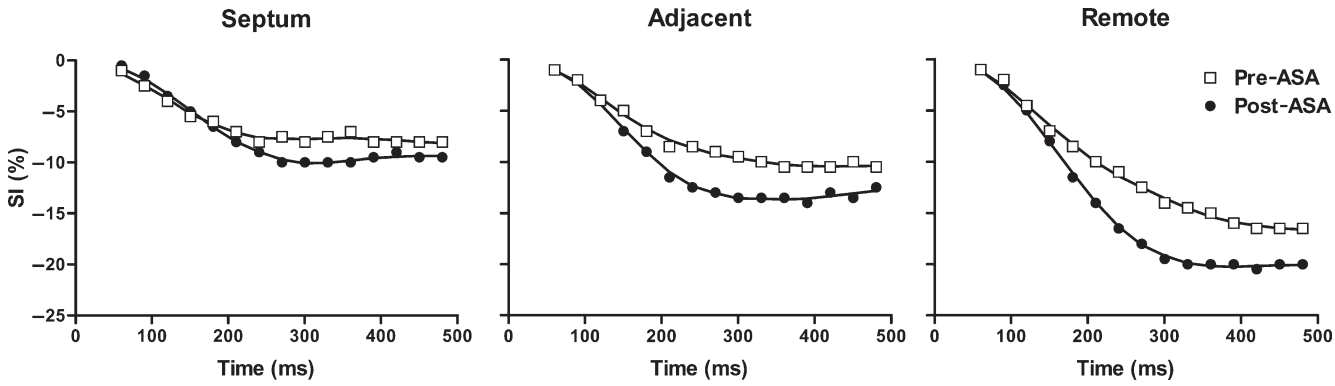

Figure 4 Typical example of regional SI strain curves in an HOCM patient pre- and post-ASA.

Table 3 Maximum systolic strain rate in septal, adjacent, and remote myocardium at baseline and 6 months after ASA in HOCM

Maximum systolic strain rate (strain/s)	Baseline	Follow-up	Δ-value	*P*-value
Antero- and inferoseptal wall				
Radial stretch rate (Err) (strain/s)	46.7 ± 22.4	48.6 ± 17.7	2.0 ± 23.1	0.953
Circumferential shortening rate (Ecc) (strain/s)	−55.2 ± 19.2	−54.2 ± 11.8	1.0 ± 13.6	0.833
Longitudinal shortening rate (Ell) (strain/s)	−35.2 ± 17.3	−41.2 ± 19.0	6.0 ± 11.6	0.159
Torsion rate (Acl) (degrees/s)	33.5 ± 10.8	29.8 ± 12.2	3.7 ± 7.4	0.214
SI rate (strain/s)	−46.8 ± 19.2	−49.5 ± 14.4	2.7 ± 8.4	0.399
Anterior and inferior wall				
Radial stretch rate (Err/s)	62.8 ± 20.2	81.5 ± 10.8	18.7 ± 16.2	0.021
Circumferential shortening rate (Ecc/s)	−72.9 ± 25.1	−81.9 ± 15.9	9.0 ± 20.2	0.236
Longitudinal shortening rate (Ell/s)	−37.5 ± 17.5	−50.5 ± 17.5	13.0 ± 6.9	0.007
Torsion rate (Acl/s) (degrees/s)	35.7 ± 9.9	42.3 ± 8.1	6.6 ± 8.2	0.028
SI rate (SI/s)	−56.5 ± 21.1	−70.0 ± 16.7	13.5 ± 11.9	0.017
Antero- and inferolateral wall				
Radial stretch rate (Err/s)	90.5 ± 17.0	111.1 ± 30.3	20.6 ± 26.2	0.049
Circumferential shortening rate (Ecc/s)	−91.9 ± 9.3	−102.3 ± 10.8	10.4 ± 11.8	0.034
Longitudinal shortening rate (Ell/s)	−42.8 ± 13.0	−62.5 ± 20.5	19.7 ± 15.3	0.012
Torsion rate (Acl/s) (degrees/s)	34.8 ± 10.0	41.7 ± 6.2	6.9 ± 11.7	0.11
SI rate (SI/s)	−70.3 ± 9.2	−86.1 ± 15.0	15.8 ± 13.9	0.011

Values expressed as mean ± SD. Δ, actual changes from baseline at 6-month follow-up.

differentiation between infarcted and non-infarcted subregions. Secondly, the difference in outcome is probably also related to the fact that their patient group was studied directly after the septal ablation procedure, at which time myocardial stunning may have played a role. In contrast, our CMR tagging data were acquired 6 months after ASA, and the improvement in function of the non-ischaemic septal myocardium may compensate for a loss of function of the infarcted septal tissue.

SI, which incorporates both circumferential and longitudinal shortening, has been introduced as a robust parameter to quantify myocardial contraction.[22] In the present study, SI tended to increase in the adjacent myocardium and improved significantly in remote myocardium at 6 months of follow-up, thereby demonstrating improved remote myocardial contraction. Similar findings were reported after afterload reduction as a result of valve replacement in patients with aortic stenosis.[27] In that study, normalization of the LV torsion and a significant increase in basal circumferential shortening were observed 12 months after surgical valve replacement. Furthermore, the increase in the circumferential shortening correlated with a decrease in the LV mass index at 1-year follow-up. This also agrees with our finding of a positive correlation between non-septal mass reduction and the per cent increase of the SI of remote myocardium at 6-month follow-up.

In a previous echocardiographic study, a decrease in the Tei index was found, a Doppler parameter reflecting both systolic and diastolic LV function, in the mid-term follow-up, indirectly suggesting improvement of myocardial performance.[12] Again, this is in agreement with the results of the current study.

Limitations

Only a limited number of patients with HOCM were studied, and the results should be interpreted with care. Nevertheless, the 3D-strain data convincingly indicate that significant changes in regional myocardial function occur in the non-infarcted (adjacent and remote) myocardial regions after ASA. Furthermore, we have chosen to aggregate the data on the patient level instead of using (for instance) multilevel analysis. This was mainly done because it improves the interpretability of the results.

In view of the limited number of patients, it must be realized that CMR tissue tagging, especially when a

four-dimensional (3-D + time) reconstruction of the LV is made, is accompanied by a time-consuming post-processing procedure. The number of tracked points within the LV wall using CMR tissue (line) tagging with a tag–tag distance of 6–7 mm is limited, which, in turn, restricts the transmural coverage of the strain calculations. More recently developed strain imaging techniques, which allow for automated strain analysis, may overcome these limitations in future studies.[28] These methods, however, were not available to us at the start of the study. Furthermore, we confined our measurements to systolic deformation, although HCM is also associated with impairment of diastolic function. Further work is needed to study the changes in diastolic function after ASA.

In conclusion, we demonstrated that reduction in remote myocardial mass after ASA was accompanied by a significant improvement of regional systolic myocardial function, supporting a concept of structural and functional reversed LV remodelling.

Acknowledgements

This study was supported by grant 99.203 from the Netherlands Heart Foundation and the Interuniversity Cardiology Institute of the Netherlands.

Conflict of interest: none declared.

References

1. Sigwart U. Non-surgical myocardial reduction for hypertrophic obstructive cardiomyopathy. *Lancet* 1995;**346**:211–214.
2. Seggewiss H, Gleichmann U, Faber L, Fassbender D, Schmidt HK, Strick C. Percutaneous transluminal septal myocardial ablation in hypertrophic obstructive cardiomyopathy: acute results and 3-month follow-up in 25 patients. *J Am Coll Cardiol* 1998;**31**:252–258.
3. Knight C, Kurbaan AS, Seggewiss H, Henein M, Gunning M, Harrington D, Fassbender D, Gleichmann U, Sigwart U. Nonsurgical septal reduction for hypertrophic obstructive cardiomyopathy: outcome in the first series of patients. *Circulation* 1997;**95**:2075–2081.
4. Lakkis NM, Nagueh SF, Kleiman NS, Killip D, He ZX, Verani MS, Roberts R, Spencer WH III. Echocardiography-guided ethanol septal reduction for hypertrophic obstructive cardiomyopathy. *Circulation* 1998;**98**:1750–1755.
5. Lakkis NM, Nagueh SF, Dunn JK, Killip D, Spencer WH III. Nonsurgical septal reduction therapy for hypertrophic obstructive cardiomyopathy: one-year follow-up. *J Am Coll Cardiol* 2000;**36**:852–855.
6. Fananapazir L, McAreavey D. Therapeutic options in patients with obstructive hypertrophic cardiomyopathy and severe drug-refractory symptoms. *J Am Coll Cardiol* 1998;**31**:259–264.
7. Roberts R, Sigwart U. New concepts in hypertrophic cardiomyopathies, part II. *Circulation* 2001;**104**:2249–2252.
8. Qin JX, Shiota T, Lever HM, Kapadia SR, Sitges M, Rubin DN, Bauer F, Greenberg NL, Agler DA, Drinko JK, Martin M, Tuzcu EM, Smedira NG, Lytle B, Thomas JD. Outcome of patients with hypertrophic obstructive cardiomyopathy after percutaneous transluminal septal myocardial ablation and septal myectomy surgery. *J Am Coll Cardiol* 2001;**38**:1994–2000.
9. Nagueh SF, Lakkis NM, He ZX, Middleton KJ, Killip D, Zoghbi WA, Quinones MA, Roberts R, Verani MS, Kleiman NS, Spencer WH III. Role of myocardial contrast echocardiography during nonsurgical septal reduction therapy for hypertrophic obstructive cardiomyopathy. *J Am Coll Cardiol* 1998;**32**:225–229.
10. van Dockum WG, ten Cate FJ, ten Berg JM, Beek AM, Twisk JWR, Vos J, Hofman MBM, Visser C, van Rossum AC. Myocardial infarction after percutaneous transluminal septal myocardial ablation in hypertrophic obstructive cardiomyopathy: evaluation by contrast-enhanced magnetic resonance imaging. *J Am Coll Cardiol* 2004;**43**:27–34.
11. van Dockum WG, Beek AM, ten Cate FJ, ten Berg JM, Bondarenko O, Götte MJW, Twisk JWR, Hofman MBM, Visser CA, van Rossum AC. Early onset and progression of left ventricular remodeling after alcohol septal ablation in hypertrophic obstructive cardiomyopathy. *Circulation* 2005;**111**:2503–2508.
12. Veselka J, Procházková Š, Bolomová-Homolová I, Duchoňová R, Tesař D. Effects of alcohol septal ablation for hypertrophic obstructive cardiomyopathy on Doppler Tei index: a mid-term follow-up. *Echocardiology* 2005;**22**:105–109.
13. Abraham TP, Nishimura RA, Holmes DR, Belohlavek M, Seward JB. Strain rate imaging for assessment of regional myocardial function. Results from a clinical model of septal ablation. *Circulation* 2002;**105**:1403–1406.
14. Zerhouni EA, Parish DM, Rogers WJ, Yang A, Shapiro EP. Human heart: tagging with MR imaging. A method for non-invasive assessment of myocardial motion. *Radiology* 1988;**169**:59–63.
15. Axel L, Dougherty L. MR imaging of motion with spatial modulation of magnetization. *Radiology* 1989;**171**:841–845.
16. Axel L, Dougherty L. Heart wall motion: improved method of spatial modulation of magnetization for MR imaging. *Radiology* 1989;**172**:349–350.
17. Marcus JT, Götte MJW, van Rossum AC, Kuijer JPA, Heethaar RM, Axel L, Visser CA. Myocardial function in infarcted and remote regions early after infarction in man: assessment by magnetic resonance tagging and strain analysis. *Magn Res Med* 1997;**38**:803–810.
18. Götte MJW, van Rossum AC, Marcus JT, Kuijer JPA, Axel L, Visser CA. Recognition of infarct localization by specific changes in intramural myocardial mechanics. *Am Heart J* 1999;**138**:1038–1045.
19. Axel L, Goncalves RC, Bloomgarden D. Regional heart wall motion: two-dimensional analysis and functional imaging with MR tagging. *Radiology* 1992;**183**:745–750.
20. Kuijer JPA, Marcus JT, Götte MJW, van Rossum AC, Heethaar RM. Three-dimensional myocardial strain analysis based on short- and long axis magnetic resonance tagged images using a 1D displacement field. *Magn Res Imaging* 2000;**18**:553–564.
21. Kim RJ, Shah DJ, Judd RM. How we perform delayed enhancement imaging. *J Cardiol Magn Reson* 2003;**5**:505–514.
22. Moore CC, Lugo-Olivieri CH, McVeigh ER, Zerhouni EA. Three-dimensional systolic strain patterns in the normal human left ventricle: characterization with tagged MR imaging. *Radiology* 2000;**214**:453–466.
23. Mazur W, Nagueh SF, Lakkis NM, Middleton KJ, Killip D, Roberts R, Spencer WH III. Regression of left ventricular hypertrophy after nonsurgical septal reduction therapy for hypertrophic obstructive cardiomyopathy. *Circulation* 2001;**103**:1492–1496.
24. Kramer CM, Reichek N, Ferrari VA, Theobald T, Dawson J, Axel L. Regional heterogeneity of function in hypertrophic cardiomyopathy. *Circulation* 1994;**90**:186–194.
25. Maier SE, Fischer SE, McKinnon GC, Hess OM, Krayenbuehl HP, Boesiger P. Evaluation of left ventricular segmental wall motion in hypertrophic cardiomyopathy with myocardial tagging. *Circulation* 1992;**86**:1919–1928.
26. Young AA, Kramer CM, Ferrari VA, Axel L, Reichek N. Three-dimensional left ventricular deformation in hypertrophic cardiomyopathy. *Circulation* 1994;**90**:854–867.
27. Sandstede JJ, Johnson T, Harre K, Beer M, Hofmann S, Pabst T, Kenn W, Völker W, Neubauer S, Hahn D. Cardiac systolic rotation and contraction before and after valve replacement for aortic stenosis: a myocardial tagging study using MR imaging. *Am J Roentgenol* 2002;**178**:953–958.
28. Zwanenburg JJM, Kuijer JPA, Marcus JT, Heethaar RM. Steady-state free precession with myocardial tagging: CSPAMM in a single breathhold. *Magn Reson Med* 2003;**49**:722–730.